Research Article

Pathogenesis of Reproductive and Metabolic PCOS Traits in a Mouse Model

Valentina Rodriguez Paris,[1] Melissa C. Edwards,[1,2] Ali Aflatounian,[1] Michael J. Bertoldo,[1] William L. Ledger,[1] David J. Handelsman,[2] Robert B. Gilchrist,[1] and Kirsty A. Walters[1,2]

[1]Fertility and Research Centre, School of Women's & Children's Health, University of New South Wales Sydney, NSW 2052, Australia; and [2]Andrology Laboratory, ANZAC Research Institute, University of Sydney, Sydney, New South Wales 2139, Australia

ORCiD numbers: 0000-0002-0880-6661 (V. Rodriguez Paris); 0000-0002-9004-6920 (A. Aflatounian); 0000-0002-9471-501X (M. J. Bertoldo); 0000-0001-6465-4343 (W. L. Ledger); 0000-0002-4200-7476 (D. J. Handelsman); 0000-0003-1611-7142 (R. B. Gilchrist); 0000-0002-1504-9734 (K. A. Walters).

Abbreviations: ALT, alanine transaminase; ANOVA, analysis of variance; AST, aspartate transaminase; DHT, dihydrotestosterone; NAFLD, nonalcoholic fatty liver disease; PCOM, polycystic ovary morphology; PCOS, polycystic ovary syndrome; SEM, standard error of the mean.

Abstract

Polycystic ovary syndrome (PCOS) is a common and heterogeneous disorder; however, the etiology and pathogenesis of PCOS are poorly understood and current management is symptom-based. Defining the pathogenesis of PCOS traits is important for developing early PCOS detection markers and new treatment strategies. Hyperandrogenism is a defining characteristic of PCOS, and studies support a role for androgen-driven actions in the development of PCOS. Therefore, we aimed to determine the temporal pattern of development of PCOS features in a well-characterized dihydrotestosterone (DHT)-induced PCOS mouse model after 2, 4, and 8 weeks of DHT exposure. Following 2 weeks of treatment, DHT induced the key PCOS reproductive features of acyclicity, anovulation, and multifollicular ovaries as well as a decrease in large antral follicle health. DHT-treated mice displayed the metabolic PCOS characteristics of increased body weight and exhibited increased visceral adiposity after 8 weeks of DHT treatment. DHT treatment also led to an increase in circulating cholesterol after 2 weeks of exposure and had an overall effect on fasting glucose levels, but not triglycerides, aspartate transaminase (AST) and alanine transaminase (ALT) levels, or hepatic steatosis. These data reveal that in this experimental PCOS mouse model, acyclicity, anovulation, and increased body weight are early features of a developing PCOS phenotype whereas adiposity, impaired glucose tolerance, dyslipidemia, and hepatic steatosis are later developing features of PCOS. These findings provide insights into the likely sequence of PCOS trait development and support the addition of body weight criteria to the early diagnosis of PCOS.

Polycystic ovary syndrome (PCOS) is the most frequent endocrine condition in women of reproductive age [1-3]. Applying the Rotterdam criteria, a woman is diagnosed with PCOS if she presents with 2 out of the 3 following traits: clinical and/or biochemical androgen excess, oligo-ovulation or anovulation, and polycystic ovarian morphology (PCOM) on ultrasound [4, 5]. However, PCOS often involves additional features affecting reproductive, endocrine, metabolic, and psychological function [5, 6]. Associated reproductive traits include luteinizing hormone hypersecretion, abnormal follicular development, reduced fertility, and an increased risk of miscarriage [2] while the adverse metabolic features comprise obesity, metabolic syndrome, hyperinsulinemia, insulin resistance, dyslipidemia, and hepatic steatosis, all of which predispose women to type 2 diabetes, cardiovascular disease, and nonalcoholic fatty liver disease (NAFLD) [2, 7-10].

Despite the high prevalence of PCOS, the etiology and pathogenesis of PCOS are poorly understood. Therefore, currently, early detection is challenging, and medical management is suboptimal as it relies solely on symptomatic treatment [3]. Establishing biomarkers for early detection requires elucidating underlying mechanisms driving PCOS and the temporal pattern of PCOS trait development. Hence, research aimed at defining the pathogenesis of PCOS traits is important for early PCOS detection and effective treatment of this disorder.

Initial features of PCOS often present during adolescence [11]. Such early diagnosis would facilitate timely diagnosis to improve management of PCOS. However, PCOS diagnosis in pubescent girls is challenging due to natural developmental changes of puberty, including irregular cycles and PCOM, making the diagnosis unreliable [12]. The international diagnostic guidelines for PCOS indicate that for diagnosis of PCOS in an adolescent, she must have both oligo-anovulation and hyperandrogenism, with PCOM not reliable for diagnosis in adolescents [4, 13]. However, some evidence supports other early diagnostic markers in young girls, aiming to better predict and possibly prevent a more severe PCOS phenotype.

The most consistent feature in women suffering with PCOS is hyperandrogenism, which is present in ~60% of patients [14]. There is now substantial experimental evidence supporting a role for androgen excess in the development of PCOS [15, 16]. Another common feature associated with PCOS is obesity [17, 18], which exacerbates PCOS features [19-21], while weight loss ameliorates them [17]. A hyperandrogenic state is associated with increased adiposity, specifically visceral adiposity, as seen in young female-to-male transgenders of healthy weight undergoing testosterone treatment which leads to a significant increase in visceral fat [22]. Moreover, a longitudinal study found that an earlier adiposity rebound (the second rise in body mass index [BMI] at 5-6 years of age) was associated with a higher BMI and PCOS diagnosis in adulthood [23]. It has been proposed that the development of PCOS might in part originate from childhood and adolescence central adiposity leading to accelerated growth and early menarche [24-26]. These findings infer that adiposity is potentially an early marker for the diagnosis of PCOS.

Unraveling the origins and temporal development of PCOS is challenging in clinical studies, due to ethical and logistical limitations. On the other hand, animal models that mimic closely PCOS features serve as valuable tools to provide insights into the underlying mechanisms driving the development of PCOS. The majority of insightful animal models of PCOS, to date, have been developed by inducing hyperandrogenism [27, 28]. In rodents, long-term exposure to DHT from peripubertal age effectively induces a wide range of endocrine, reproductive, and metabolic features of PCOS, making it an ideal model for experimental studies of PCOS pathogenesis [29-33]. Therefore, the objective of the present study was to investigate the pathogenesis of PCOS by analyzing the temporal pattern of hyperandrogenic-induced PCOS trait development using a well-characterized PCOS mouse model.

Methods

Mice and Experimental Design

A total of 36 3-week-old C57BL/6J female mice were purchased and housed at the Biological Resources Centre facility at UNSW (Sydney, Australia). Mice were housed in groups of 3 per cage and maintained under standard housing conditions with ad libitum access to food and water in a temperature- and humidity-controlled, 12-hour light/dark environment. After a 1-week acclimatization period, PCOS-like traits were established using a previously validated method [30, 34]. Briefly, peripubertal (4-week-old) female mice were implanted subcutaneously with either an empty blank (control, 18 mice) or a dihydrotestosterone (DHT, 18 mice) 1-cm silastic implant (id, 1.47 mm; od, 1.95 mm, Dow Corning Corp, catalog no. 508–006). The DHT silastic implants are made in-house, contain ~10 mg DHT and provide

steady-state DHT release for at least 6 months [35]. This method provides elevated circulating levels of DHT, as consistently demonstrated in previous studies [30, 36, 37]. Groups of 6 control and 6 DHT-treated mice were collected following 2, 4, and 8 weeks of DHT exposure. This experiment was approved by the Animal Care and Ethics Committee of the University of New South Wales Sydney within National Health and Medical Research Council guidelines for animal experimentation.

Assessment of Estrous Cycle

Estrous-cycle stage was determined in all mice by assessing vaginal epithelial cell smears taken every day for 7 consecutive days [38]. Smears were collected using 15 µL of 0.9% sterile saline, transferred to glass slides to air dry, and stained with 0.5% toluidine blue before examination under a light microscope. Estrous-cycle stage was determined based on the presence or absence of leukocytes, cornified epithelial cells, and nucleated epithelial cells. Proestrus was characterized by the presence of mainly nucleated and some cornified epithelial cells; at the estrus stage, mostly cornified epithelial cells were present; at metestrus, both cornified epithelial cells and leukocytes were present; and at diestrus, primarily leukocytes were present.

Ovary Preparation and Morphological Analysis

Ovarian morphology analysis was performed on 16 control and 18 DHT-treated ovaries (4-6 ovaries per treatment/time point). Ovaries were dissected, weighed, fixed in 4% (weight/vol) paraformaldehyde overnight at 4 °C, and stored in 70% (vol/vol) ethanol before histological processing and analysis. Ovaries were processed through graded alcohols and embedded in glycol methacrylate resin (Technovit 7100; Heraeus Kulzer). Embedded ovaries were sectioned at 20 µm, stained with periodic acid-Schiff, and counterstained with hematoxylin. Corpora lutea quantification was undertaken as previous described [32, 39], where whole-section scans of every third section were taken under a light microscope using a DP70 Olympus camera and corpora lutea identified by morphological properties consistent with luteinized follicles and visible through several serial sections. Large antral follicles were assessed on all ovarian sections and were classified as containing a single large antrum. Follicles were only assessed in the section where the oocyte's nucleolus was evident to avoid counting repetition. Large antral follicles were classified as unhealthy if they contained a degenerate oocyte and/or more than 10% of the granulosa cells were pyknotic in appearance [32, 40]. Large antral follicles were evaluated for granulosa

cell-layer thickness and theca cell area using ImageJ version 1.48 software (NIH), as previously described [32].

Adipose Tissue Analysis

Parametrial fat pads were weighed, fixed in 4% paraformaldehyde, embedded in paraffin, and sectioned at 8 µm. Sections were stained with hematoxylin and eosin and imaged at 40× magnification under an Olympus BX60 light microscope for histomorphometric analysis. For proper representation of the fat pad, 5 distinct pictures were taken from each of 3 sections of the fat pad, with a minimum of 200 µm separating these sections. Parametrial adipocyte size was quantified using ImageJ version 1.51 software (NIH).

Cholesterol and Triglyceride Levels

Serum levels of total cholesterol and triglyceride were assayed enzymatically with commercial kits obtained from Wako (Cholesterol E Kit, 439–17501; Triglyceride Kit, 432–40201).

Fasting Glucose Levels and Glucose Tolerance Test

Fasting glucose levels and intraperitoneal glucose tolerance test were measured in all mice 1 week prior to the collection time point (ie, at 1, 3, and 7 weeks). Mice were fasted for 6 hours for a baseline blood glucose reading, followed by an intraperitoneal injection of glucose at 2 g/kg body weight. Blood glucose was then measured at 15, 30, 60, and 90 minutes post injection. Blood was obtained from a tail prick, and blood glucose levels were measured using glucose strips on an Accu-Chek glucometer (Roche).

Aspartate Transaminase and Alanine Transaminase Levels

Serum aspartate transaminase (AST) and alanine transaminase (ALT) levels were assayed enzymatically with commercial kits obtained from Thermo Scientific (ALT/GPT Reagent, TR71121; AST/GOT Reagent, TR70121).

Hepatic Steatosis Analysis

Livers were weighed whole before the right lateral lobe was excised from the whole liver and fixed in 4% paraformaldehyde, embedded in paraffin, sectioned at 5 µm, and stained with hematoxylin and eosin before histomorphometric analysis. The presence of steatosis was microscopically quantified blindly by an independent investigator by classification into

4 different categories (0, nonfatty liver; 1, possible early steatosis; 2, moderate steatosis; 3, severe steatosis; as outlined in a previous study [41]).

Statistical Modeling and Analysis

Statistical analysis was performed using GraphPad Prism 8. Proportions were analyzed by Fisher exact test to assess the effect of DHT treatment for percentage of females cycling. Statistical differences were tested by 2-way analysis of variance (ANOVA) (to assess the main effects of DHT treatment (D), time of exposure (T), and the interaction of treatment × time [D × T]), with post hoc test using Fisher least significant difference multiple comparison test. Two-way ANOVA main effects of DHT treatment (D) and time of exposure (T) are reported, and interaction results (D × T) were excluded if not significant. Data that were not normally distributed were analyzed using the Kruskal-Wallis test with uncorrected Dunn's multiple comparison test. P values < 0.05 were considered statistically significant.

Results

Disruption of Estrous Cycles Is an Early Indicator of the Development of a PCOS-Like Phenotype in a Hyperandrogenic PCOS Mouse Model

The presence of irregular menstrual cycles is a key diagnostic trait of PCOS [4, 5]. At all time points assessed, 100% of control mice cycled and displayed normal estrous-cycle patterns (Fig. 1A-1C). In contrast, acyclicity was observed in all DHT-treated mice after 2, 4, and 8 weeks of exposure to androgen excess (Fig. 1A, $P < 0.05$; and Fig. 1C). Examination of vaginal smears revealed leukocytes to be the main cell type present in all the vaginal smears from DHT-treated mice, indicating that they were in a pseudo-diestrus acyclic state (Fig. 1B and 1C).

Polycystic Ovary Morphology and Ovulatory Dysfunction Are Early Indicators of the Development of a PCOS-Like Phenotype in a Hyperandrogenic PCOS Mouse Model

In agreement with our previous studies [30, 32], DHT treatment led to a significant increase in the large antral follicle population and prevented ovulation (Fig. 2A and 2B and 2D and 2E, $P < 0.001$). Similarly, histological analysis revealed that DHT treatment had an overall significant effect on the number of cyst-like follicles in the ovaries ($P < 0.05$), with DHT-treated ovaries displaying an increase in the number of cyst-like follicles compared with controls after 2, 4, and 8 weeks of excess androgen exposure (Fig. 2C).

DHT-exposed females also displayed the PCOS trait of oligo/anovulation, with DHT treatment leading to a significant decrease in corpora lutea (Fig. 2D and 2E, $P < 0.05$). Corpora lutea were notably decreased in DHT-treated mice compared with controls after 2 weeks of exposure to excess androgen levels, and completely diminished after 4 and 8 weeks (Fig. 2A and 2D). Time had a significant main effect on ovary weight ($P < 0.001$), but there was no main effect of DHT treatment (Fig. 2F).

Ovarian Antral Follicle Health and Morphology Are Significantly Compromised After 2 Weeks of Excess Androgen Exposure in a Hyperandrogenic PCOS Mouse Model

A significant effect of DHT treatment was identified for the PCOS-like ovarian feature of an increased number of atretic large antral follicles (Fig. 3A and 3B, $P < 0.05$), with DHT-treated females displaying an increase in the percentage of unhealthy large antral follicles after just 2 weeks of DHT exposure. Excess androgen exposure also had an overall significant (2-way ANOVA, main effect; $P < 0.05$) effect on granulosa cell thickness (Fig. 3C). Granulosa cell thickness was observed to decrease in large antral follicles of DHT-treated mice compared to controls after 2, 4, and 8 weeks of exposure, (Fig. 3C). DHT treatment and time of exposure had no effect on theca cell area (Fig. 3D).

Increased Body Weight Is an Early Marker of the Development of a PCOS-Like Phenotype in a Hyperandrogenic PCOS Mouse Model

In line with our previous studies [30, 32], DHT treatment had a significant impact on body weight ($P < 0.001$). DHT-treated mice displayed increased body weights compared with control females following 2, 4, and 8 weeks of androgen exposure (Fig. 4A), with body weight increasing in all treatment groups over time (Fig. 4A, $P < 0.05$). Body weight in DHT-treated females was increased by 18% after 2 and 4 weeks of DHT exposure and by a further 12% at 8 weeks of DHT exposure compared with controls. Increased visceral adiposity is a characteristic of women with PCOS [42] and correspondingly we observed that DHT treatment induced a significant increase in parametrial ($P < 0.001$) and retroperitoneal fat pad ($P < 0.001$) weights after 8 weeks of excess androgen exposure, compared with controls (Fig. 4B and 4C). Mesenteric fat pad weight was significantly influenced by time ($P < 0.01$) but not DHT treatment (Fig. 4D). Inguinal and brown fat pad weights were not affected by either time or DHT treatment (Fig. 4E and 4F). Histological analysis of parametrial adipocyte size revealed that time
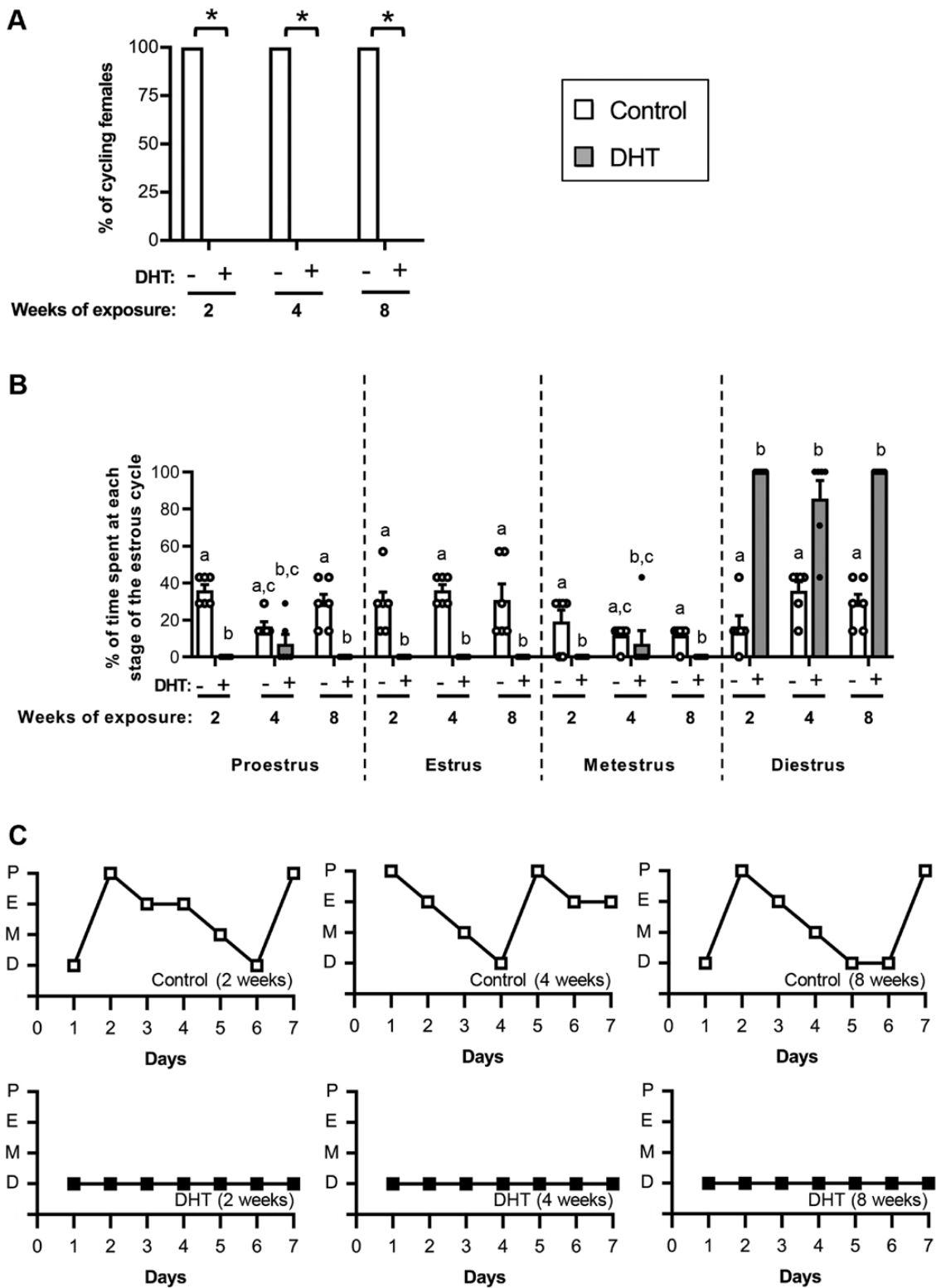
Figure 1. Estrous cycles in DHT-induced PCOS mice are disrupted after 1 week of exposure to androgen excess. **A,** Percentage of females cycling in a 1-week period. *Significant effect of DHT identified by Fisher exact test ($P < 0.05$). n = 6 mice/group. **B,** Proportion of time spent at each stage of the estrous cycle, showing significantly altered estrous cycles in DHT-exposed mice after 2, 4, and 8 weeks of androgen exposure. n = 6 mice/group. Data are the mean ± standard error of the mean (SEM) (n = 6 mice/group). Different letters denote significant statistical difference; Kruskal-Wallis test followed by Uncorrected Dunn's multiple comparison test. **C,** Representative graphs of estrous cycle pattern in control and DHT-treated females after 2, 4, and 8 weeks of androgen exposure. Abbreviations: P, proestrus; E, estrus; M, metestrus; D, diestrus. Data are the mean ± SEM (n = 6 mice/group).
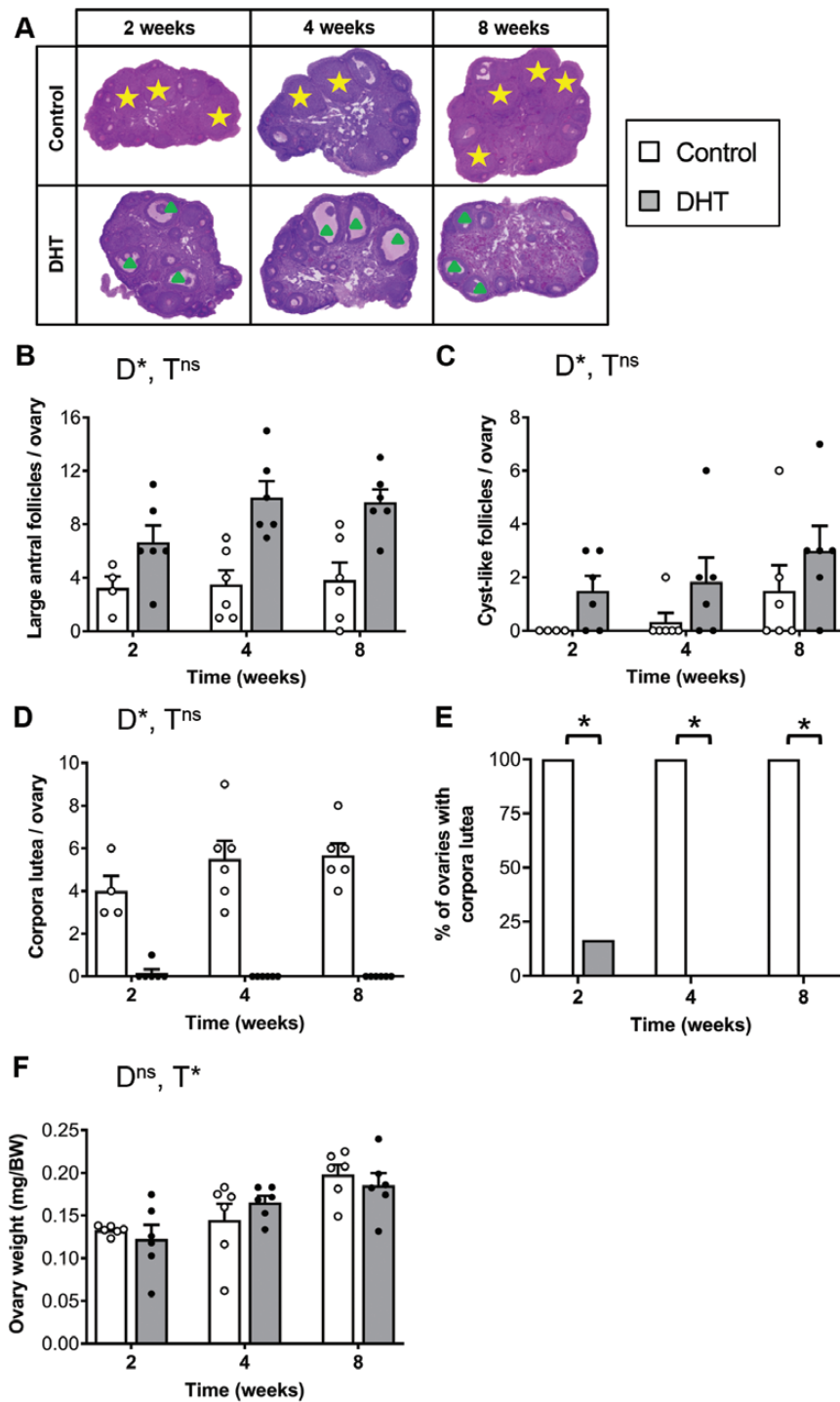
Figure 2. Polycystic ovary morphology (PCOM) and ovulatory dysfunction is present after 2 weeks of androgen exposure. **A**, Histological sections of representative ovaries from each group. Yellow star, corpora lutea; green triangle, arrested large antral follicle. **B**, Average number of large antral follicles per ovary showing a significant effect of DHT treatment ($P < 0.001$, 2-way ANOVA). Data are the mean ± SEM (n = 4-6 ovaries/group). **C**, Average number of cyst-like follicles per ovary (DHT treatment main effect $P < 0.05$, 2-way ANOVA). Data are the mean ± SEM (n = 4-6 ovaries/group). **D**, Average number of corpora lutea (CL) per ovary showing a significant effect of DHT treatment ($P < 0.001$, 2-way ANOVA). Data are the mean ± SEM (n = 4-6 ovaries/group). **E**, Percentage of ovaries with CL, showing a significant effect of DHT identified by Fisher exact test ($P < 0.05$). n = 4-6 ovaries/group. **F**, Average ovary weight (time main effect $P < 0.05$, 2-way ANOVA). Data are the mean ± SEM (n = 12 ovaries/group). Abbreviations: D, DHT; ns, no significant difference; T, time. *$P < 0.05$, 2-way ANOVA.
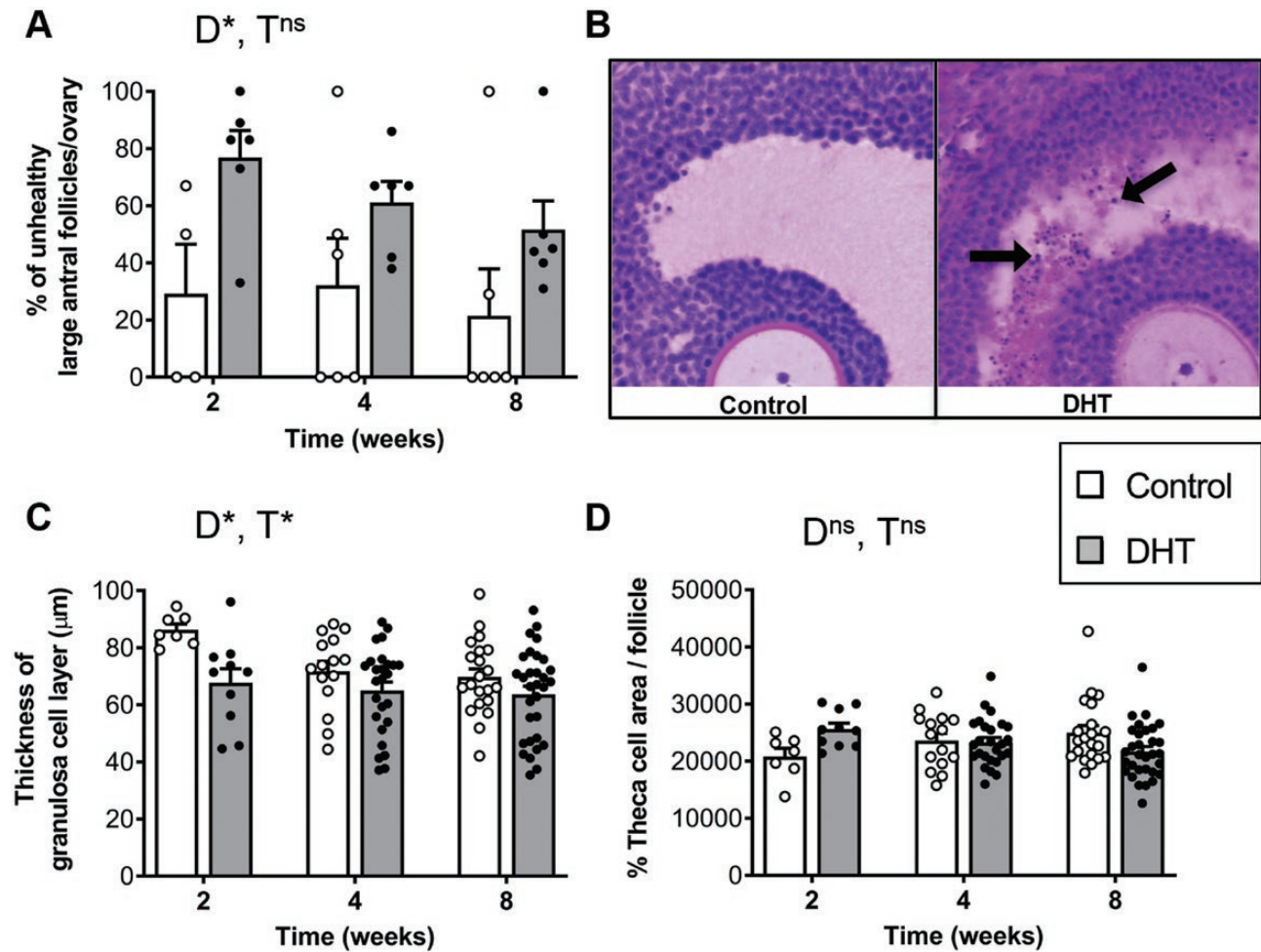
Figure 3. DHT treatment significantly alters follicle health and granulosa cell thickness after 2 weeks of treatment. **A**, Percentage of unhealthy large antral follicles per ovary showing a significant effect for DHT treatment ($P < 0.05$, 2-way ANOVA). Data are the mean ± SEM (n = 4-6 ovaries/group). **B**, Histological cross-section of representative antral follicles, showing the presence of pyknotic cells (black arrows) within the granulosa cell layer of DHT-treated mice. **C**, Average thickness of granulosa cell layer per follicle showing a significant effect for DHT treatment ($P < 0.05$, 2-way ANOVA). Data are the mean ± SEM (n = 7-31 follicles/group). **D**, Average percentage of theca cell area per follicle showing no significant effect of DHT treatment or time ($P = 0.3$, 2-way ANOVA). Data are the mean ± SEM (n = 7-31 follicles/group). Abbreviations: D, DHT; ns, no significant difference; T, time; *$P < 0.05$, 2-way ANOVA.

($P < 0.001$), but not DHT, had a significant effect on adipocyte size (Fig. 4G and 4H).

Excess Androgen Exposure Induced an Increase in Cholesterol Levels and Basal Glucose Levels in a Hyperandrogenic PCOS Mouse Model

Dyslipidemia, an abnormal amount of lipids such as cholesterol and triglycerides in circulation, is prevalent in women with PCOS and can predispose women to suffer from cardiovascular disease [43]. In this study, DHT treatment, but not time, had a significant effect on total cholesterol levels ($P < 0.001$); as compared with controls, DHT-treated females displayed a 94% and a 43% increase after 2 ($P < 0.001$) and 8 ($P < 0.05$) weeks of androgen excess exposure, respectively (Fig. 5A). Circulating triglyceride levels

were not affected by either DHT treatment or time (Fig. 5B). Serum fasting glucose levels were significantly affected by DHT treatment ($P < 0.05$) and time ($P < 0.001$), with levels observed to increase over time with highest levels observed in DHT-treated mice after 8 weeks of androgen exposure compared with controls (control, 9.03 ± 0.34 mmol/L vs DHT, 10.57 ± 0.42 mmol/L; Fig. 5C). However, overall glucose tolerance was unaffected by either time or DHT treatment (Fig. 5D).

Liver Damage Is Not Apparent During the Early Stages of Exposure to Excess Androgens in a Hyperandrogenic PCOS Mouse Model

To assess liver function, we measured the enzymes aspartate transaminase (AST) and alanine transaminase
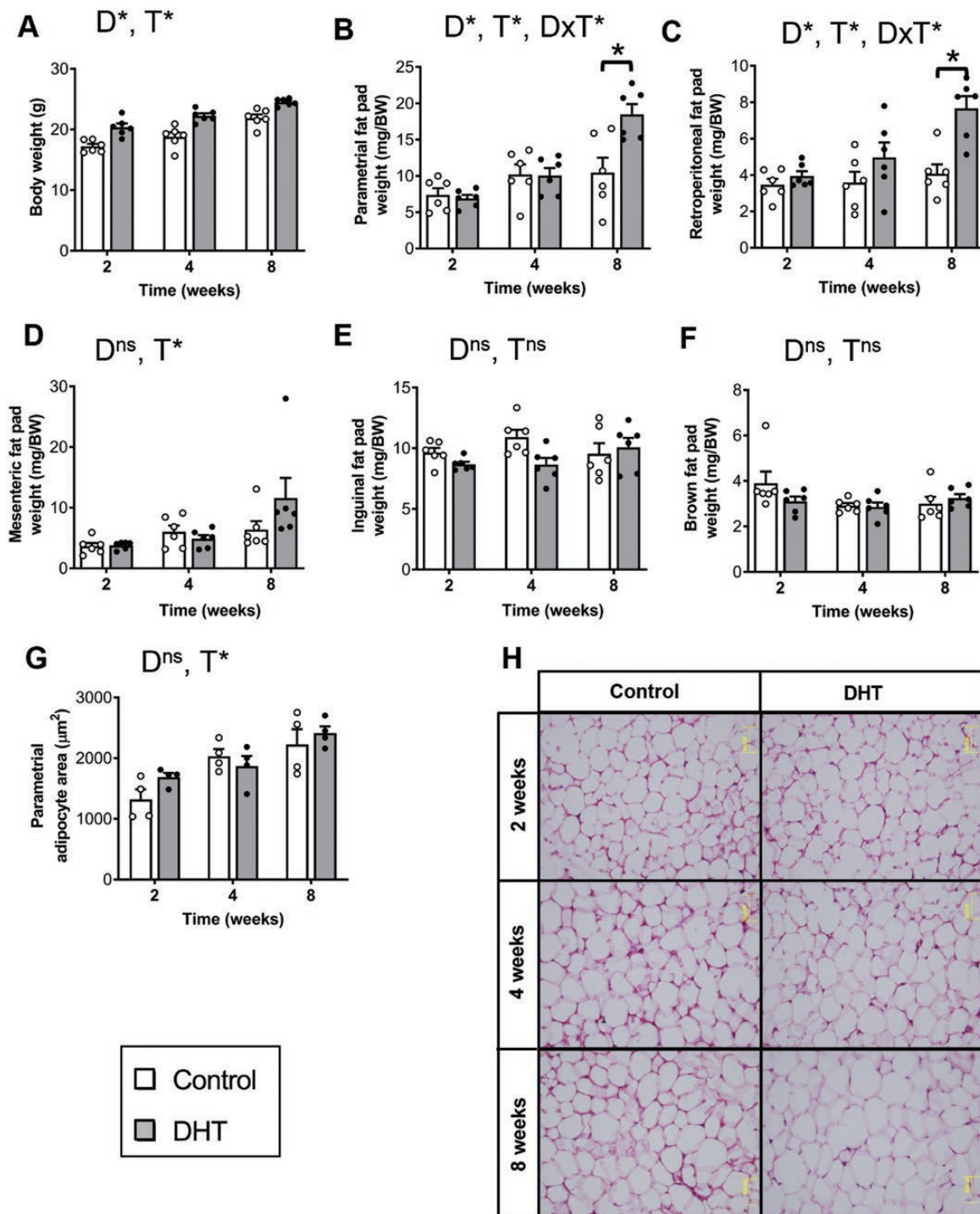
Figure 4. Body weight is increased after 2 weeks of androgen exposure. **A**, Average body weight indicating a significant effect of DHT treatment (*P* < 0.001, 2-way ANOVA). Data are the mean ± SEM (n = 6 mice/group). Average parametrial (**B**) and retroperitoneal (**C**) fat pad weights showing a significant effect of DHT treatment after 8 weeks of exposure (both *P* < 0.001, 2-way ANOVA). Data are the mean ± SEM (n = 6 mice/group). Average mesenteric (**D**) inguinal (**E**) and brown (**F**) fat pad weights showing no significant effect of DHT treatment (all *P* > 0.05, 2-way ANOVA). **G**, Average adipocyte size of parametrial fat pad. Data are the mean ± SEM (n = 4 mice/group). **H**, Histological sections of representative parametrial fat pads from each treatment group. Abbreviations: D, DHT; ns, no significant difference; T, time; *P* < 0.05, 2-way ANOVA.

(ALT), since increased levels in circulation are associated with liver damage [44]. Neither DHT treatment or time exerted a significant effect over ALT and AST levels at any time point (Fig. 5E and 5F), indicating that DHT treatment did not cause liver damage during the early stages of PCOS development in this model. Histological analysis also showed there was no significant difference in the degree of liver steatosis observed between control
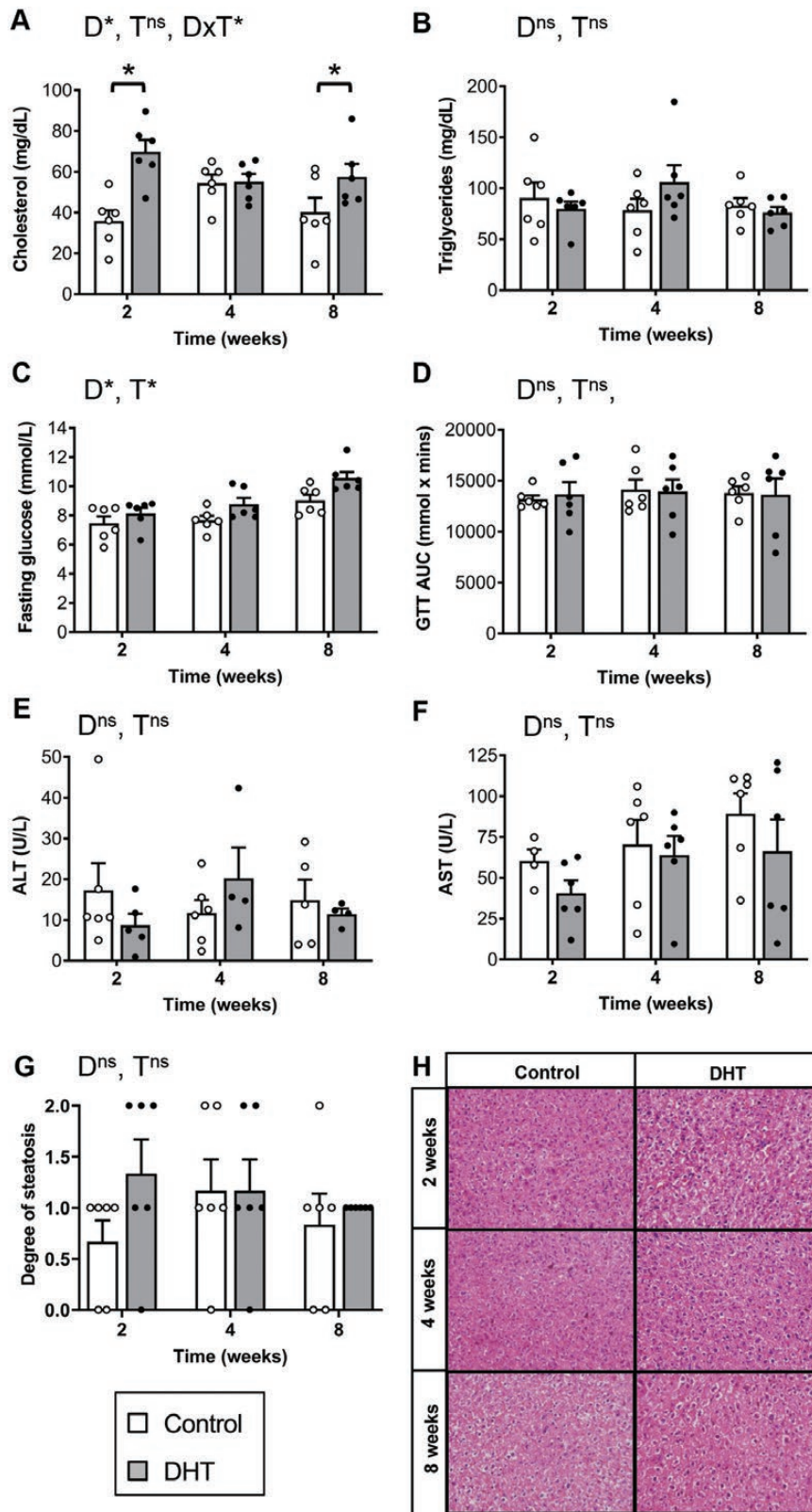
Figure 5. Serum cholesterol, triglyceride, and fasting glucose levels, glucose tolerance tests, and aspartate transaminase (AST) and alanine transaminase (ALT) liver function marker measurements. **A**, Serum total cholesterol demonstrating a significant increase in cholesterol levels at 2 and 8 weeks post-DHT treatment exposure ($P < 0.05$, 2-way ANOVA). Data are the mean ± SEM ($n = 6$ mice/group). **B**, Serum total triglyceride levels displaying no significant effect of DHT treatments ($P = 0.7$, 2-way ANOVA). Data are the mean ± SEM ($n = 6$ mice/group). **C**, 6-hour serum fasting glucose levels showing a significant effect of DHT treatment ($P < 0.05$, 2-way ANOVA). Data are the mean ± SEM ($n = 6$ mice/group) **D**, glucose tolerance test (GTT) area under the curve (AUC), showing DHT treatment had no effect over clearance of glucose in the circulation ($P = 0.9$, 2-way ANOVA). Data

and DHT-treated mice following up to 8 weeks of DHT exposure (Fig. 5G and 5H).

Discussion

The current international criteria for the diagnosis of PCOS are based on the diagnosis of adult women and may not be equally applicable to adolescents [4]. PCOS diagnosis during puberty is challenging, due to the fact that irregular menstrual cycles, acne, mild hyperandrogenism, and multifollicular ovarian morphology occur during normal puberty, which consequently makes diagnosis unreliable [11-13]. Therefore, diagnosis is often deferred and reassessed many years after menarche [4] to avoid overdiagnosis, needless anxiety, and unwarranted interventions. The establishment of the natural history of PCOS progression could assist in identifying markers for the early detection of PCOS. These would be beneficial in providing more accurate criteria for early diagnosis of PCOS. The present study investigated the evolution of PCOS features in an established hyperandrogenic PCOS mouse model and identified that the appearance of the PCOS reproductive traits of acyclicity and anovulation, and the PCOS metabolic trait of increased body weight were the earliest to develop followed by increased adiposity. However, other PCOS-associated metabolic features did not develop and thus are proposed to occur after a longer period of time as observed in our previous publications. Our data support the use of irregular cycles and also the addition of elevated body weight as early diagnostic criteria in adolescence for predicting the likelihood of developing PCOS in adulthood.

Substantial evidence points to hyperandrogenism playing a causative role in the development of PCOS traits [30, 32]. The majority of women presenting with PCOS exhibit elevated levels of androgens [14], and hyperandrogenism correlates closely with the main features of PCOS [45]. Yet the temporal order by which hyperandrogenic-mediated traits develop is unknown. In the current study, estrous cyclicity was disrupted after only 2 weeks of exposure to androgen excess and vaginal smears revealed that independent of the length of time of DHT exposure, DHT-treated female mice were fixed in a pseudo-diestrus state of their cycle. This finding corresponds with previous observations in healthy adolescent girls where irregular menstrual cycles during early puberty are associated with higher free testosterone

to free 17β-estradiol ratios, in comparison with mid- and late puberty [46]. Indeed, it has been hypothesized that PCOS may arise from abnormal pubertal development [46]. This concept is supported by the finding in the current study, where a hyperandrogenic environment from the peripubertal stage completely disrupted hormonal balance causing cessation of estrous cycling in DHT-treated mice. This finding indicates that irregularity of cycles, although present in the early stages of puberty, is also an important factor that may help identify early stages of PCOS in the first years after menarche.

Women with PCOS exhibit an increase in antral follicles leading to the development of PCOM ovaries and oligo-anovulation [4]. Both characteristics were effectively induced in the DHT-induced PCOS mouse model. DHT exposure led to oligo/anovulation after just 2 weeks of excess androgen exposure corresponding with early puberty in the mouse; likewise, PCOM developed after 2 weeks of androgen excess (6 weeks of age). This ovarian phenotype is in line with previous studies using DHT-induced PCOS rodent models [29, 31, 32], and indicates that a hyperandrogenic environment during peripuberty leads to rapid changes in ovarian morphology and ovarian function. Moreover, our results support the current PCOS guidelines for assessment of PCOS in adolescents, in which diagnosis is based on acyclicity and oligo-anovulation, with lesser weight given to establishment of PCOM for diagnosis. In agreement with previous reports, excess androgen exposure also compromised ovarian follicle health and morphology [29, 31-33], leading to a higher percentage of unhealthy large antral follicles. This increased incidence of unhealthy follicles may be attributed to the hyperandrogenic environment altering follicular dynamics [33]. Findings in the present study demonstrate that androgen excess leads to an immediate impairment of follicle health and morphology during early puberty; this therefore encourages close monitoring of PCOM in the early stages of PCOS diagnosis. In our previous study, we demonstrated that a hyperandrogenic environment was capable of altering follicular dynamics even after follicles were removed from the hyperandrogenic environment and cultured in vitro [33], indicating that a hyperandrogenic environment might play a causative role in antral follicle arrest leading to polycystic ovaries. Therefore, we propose that, in the presence of hyperandrogenism, PCOM could be included as a PCOS diagnostic feature in adolescents. However, it should be

---

Figure 5: continued

are the mean ± SEM (n = 6 mice/group). Serum ALT (**E**) and AST (**F**) levels showing no significant effect of DHT treatment ($P = 0.8$ and $P = 0.2$, 2-way ANOVA). Data are the mean ± SEM (n = 4-6 mice/group). **G**, Degree of liver steatosis showing no significant effect of DHT treatment ($P = 0.21$, 2-way ANOVA). Data are the mean ± SEM (n = 6 mice/group). **H**, Hematoxylin and eosin–stained histological sections of representative liver sections from each treatment group. Abbreviations: D, DHT; T, time; ns, no significant difference; *$P < 0.05$, 2-way ANOVA.

noted that, as rodents are poly-ovulatory, this species extrapolation must be viewed with caution.

Long-term exposure of mice to DHT from the peripubertal stage is reported to induce several metabolic features of PCOS, including increased body weight and adiposity [30, 32]. In this study, the first PCOS-like metabolic trait to be observed after DHT treatment was an increase in body weight. Although we did not quantify lean body mass, this increase in body weight is likely due to an increase in lean body mass, previously reported in this mouse model [32, 37], as mice did not display significant increases in fat depot weights until 8 weeks of DHT treatment. After 8 weeks of androgen exposure, when mice are mature adults, a significant increase in parametrial and retroperitoneal fat pad weights, representing visceral fat, was observed. This finding demonstrates that elevated androgen levels lead to an increase in adiposity that reached significance in early adulthood. Similarly, it was reported that 18- to 21-year-old daughters of women with PCOS exhibit a significant increase in BMI and waist circumference compared with daughters born to control women [47]. Moreover, 71% of the daughters with PCOS mothers were diagnosed with hyperandrogenic PCOS [47]. In the current study, DHT was observed to cause an increase in visceral fat pads, and correspondingly, patients with PCOS were reported to display a significant increase in visceral adiposity, which was positively correlated with circulating androgen levels [48]. Interestingly, this increase in visceral adiposity did not result in a significant difference in overall adiposity and body weight between healthy controls and women with PCOS, pointing to preferential fat deposition [48]. In addition, an increased amount of visceral fat has been identified to be a significant variable correlating with metabolic dysfunction in women with PCOS [49]. Collectively, these findings suggest that along with the current PCOS diagnostic criteria, close monitoring of body weight increments and fat localization in adolescents may be an additional early predictor of PCOS.

The severity of obesity in adolescent girls increases the odds of PCOS [50]. This notion is supported by a longitudinal study analyzing data from the Northern Finland Birth Cohort (NFBC) of 1966 reporting that women with abdominal obesity who were overweight or obese at ages 14 and 31 displayed an increased risk of PCOS [51]. A more recent analysis of the same cohort revealed that girls who exhibited an earlier adiposity rebound at 5 to 6 years of age correlated with PCOS diagnosis and a higher BMI in adulthood [23]. Thus, these findings demonstrate that an increase in adiposity early in life is an indicator of increased likelihood of PCOS diagnosis later in life—although not a certainty, given the rise in obesity in children and adolescents worldwide [52], and thus caution must be employed

to avoid overdiagnosis. Taken together, these findings suggest that the development of strategies to prevent this increase in adiposity at an early stage may be a key preventative treatment, as obesity is known to exacerbate the metabolic phenotype observed in women with PCOS [19], increasing their risk for cardiovascular disease risk factors such as glucose intolerance and dyslipidemia [53].

Dyslipidemia is prevalent in women with PCOS and can predispose women to suffer from cardiovascular disease [43]. In this study, DHT exposure significantly influenced total cholesterol levels, with an overall increase in cholesterol levels in DHT-treated female mice compared with controls. Similarly, a study reported that obese adolescents with PCOS displayed significantly higher total cholesterol levels when compared with healthy weight non-PCOS adolescents [54]. However, in the current study, variability was observed at different time points, suggesting that, as observed in women with PCOS [55], dyslipidemia is a variable feature with some individuals displaying greater sensitivity than others. For example, a study in obese adolescents reported no significant difference in total cholesterol levels between obese adolescents with PCOS and obese adolescents without PCOS [56, 57]. Confirming previous reports [30, 32], impaired glucose homeostasis after DHT exposure was observed in the present study. This result is congruent with human studies that report increased levels of fasting glucose in women with PCOS compared with healthy women [58]. Of note, elevated levels of fasting glucose are used to define prediabetes and diabetes [59]. Therefore, in the current study, DHT-treated mice could be classified as being prediabetic, as they exhibited elevated fasting glucose levels. Notably, some studies have found a strong correlation between visceral adiposity and insulin resistance in women with PCOS, hypothesizing that visceral fat potentially causes insulin resistance [49]. In light of this knowledge, from this current study it may be hypothesized that increased visceral adiposity most likely precedes the metabolic PCOS feature of insulin resistance as, although fasting blood glucose was affected by DHT treatment, abnormal glucose intolerance was not observed up to 8 weeks of excess androgen exposure. These results further support that early lifestyle interventions to prevent an increase in adiposity are key to avert the onset of further metabolic derangements such as diabetes and cardiovascular disease.

There is an increased rate of nonalcoholic fatty liver disease (NAFLD) in women and adolescents with PCOS [60, 61]. An early feature of NAFLD is hepatic steatosis in the liver, which has been consistently induced by androgen excess in the PCOS mouse model used in this study [30, 32]. In the current study, we did not observe a significant difference in degree of hepatic steatosis in control and DHT-treated mice, whereas we do when mice are exposed to 12

Figure 6. Summary of the temporal effects of excess androgen exposure in the development of PCOS-like traits. ✓ = Clinical PCOS trait present; ✗ = Clinical PCOS trait not present. #DHT treatment induced a significant main effect which was visualized from 2 weeks of exposure. *Data for 12 weeks of androgen excess exposure are taken from our previous publications, (Caldwell 2014, 2017; Bertoldo 2019; Aflatounian 2020).

weeks of DHT [32, 33, 36], suggesting this feature is developed after a more prolonged period of excess androgen exposure (Fig. 6). Increased levels of ALT, and to a lesser degree AST, in serum are common indicators of underlying NAFLD [62] and are reported to be significantly elevated in women with PCOS [63]. However, in the current study we did not observe significantly elevated levels of ALT or AST in serum of DHT-treated mice compared with controls. This suggests that the liver was not significantly damaged at this stage in the DHT-treated females. These results indicate that the increased risk women with hyperandrogenic PCOS have of experiencing NAFLD is a long-term consequence and altered liver function and hepatic steatosis are unlikely to serve as early diagnostic factors for the diagnosis of PCOS in adolescents (Fig. 6).

In this study we present the temporal pattern of PCOS trait development in a hyperandrogenic PCOS mouse model. Findings show that acyclicity, anovulation, and increased body weight are the first PCOS-like features to occur when inducing PCOS traits through hyperandrogenism. We propose that along with the current diagnostic criteria of irregular cycles and dysfunctional ovulations, the presence of elevated body weight

and waist circumference may also be useful early markers of PCOS. Interestingly, a significant increase in visceral adiposity was not observed until a longer exposure duration of androgen excess, and glucose intolerance did not develop in the 8-week period; hence, potentially these features could be prevented. Indeed, prevention of significant increases in body weight would decrease the incidence and risk of women suffering from PCOS to develop the associated comorbidities such as cardiovascular disease and type 2 diabetes. Overall, these findings support the development of treatments that are aimed at targeting hyperandrogenic driven mechanisms and also indicate that accompanying lifestyle interventions such as diet and exercise aimed at prevention or amelioration of excess weight gain during adolescence may prove to be beneficial treatment strategies for PCOS.

Acknowledgments

Additional Information

References

1. March WA, Moore VM, Willson KJ, Phillips DI, Norman RJ, Davies MJ. The prevalence of polycystic ovary syndrome in a community sample assessed under contrasting diagnostic criteria. *Hum Reprod.* 2010;**25**(2):544-551.

2. Dumesic DA, Oberfield SE, Stener-Victorin E, Marshall JC, Laven JS, Legro RS. Scientific statement on the diagnostic criteria, epidemiology, pathophysiology, and molecular genetics of polycystic ovary syndrome. *Endocr Rev.* 2015;**36**(5):487-525.

3. Escobar-Morreale HF. Polycystic ovary syndrome: definition, aetiology, diagnosis and treatment. *Nat Rev Endocrinol.* 2018;**14**(5):270-284.

4. Teede HJ, Misso ML, Costello MF, et al.; International PCOS Network. Recommendations from the international evidence-based guideline for the assessment and management of polycystic ovary syndrome. *Hum Reprod.* 2018;**33**(9):1602-1618.

5. The Rotterdam ESHRE/ASRM-Sponsored PCOS Consensus Workshop Group. Revised 2003 consensus on diagnostic criteria and long-term health risks related to polycystic ovary syndrome (PCOS). *Hum Reproduct.* 2004;**19**(1):41-47.

6. Dokras A, Saini S, Gibson-Helm M, Schulkin J, Cooney L, Teede H. Gaps in knowledge among physicians regarding diagnostic criteria and management of polycystic ovary syndrome. *Fertil Steril.* 2017;**107**(6):1380-1386.e1.

7. Joham AE, Palomba S, Hart R. Polycystic ovary syndrome, obesity, and pregnancy. *Semin Reprod Med.* 2016;**34**(2):93-101.

8. Shorakae S, Boyle J, Teede H. Polycystic ovary syndrome: a common hormonal condition with major metabolic sequelae that physicians should know about. *Intern Med J.* 2014;**44**(8):720-726.

9. Glintborg D, Rubin KH, Nybo M, Abrahamsen B, Andersen M. Cardiovascular disease in a nationwide population of Danish women with polycystic ovary syndrome. *Cardiovasc Diabetol.* 2018;**17**(1):37.

10. Rubin KH, Glintborg D, Nybo M, Abrahamsen B, Andersen M. Development and risk factors of type 2 diabetes in a nationwide population of women with polycystic ovary syndrome. *J Clin Endocrinol Metab.* 2017;**102**(10):3848-3857.

11. Witchel SF, Oberfield SE, Peña AS. Polycystic ovary syndrome: pathophysiology, presentation, and treatment with emphasis on adolescent girls. *J Endocr Soc.* 2019;**3**(8):1545-1573.

12. Witchel SF, Oberfield S, Rosenfield RL, et al. The diagnosis of polycystic ovary syndrome during adolescence. *Horm Res Paediatr.* 2015;**83**(6):376-389.

13. Peña AS, Witchel SF, Hoeger KM, et al. Adolescent polycystic ovary syndrome according to the international evidence-based guideline. *BMC Med.* 2020;**18**(1):72.

14. Livadas S, Pappas C, Karachalios A, et al. Prevalence and impact of hyperandrogenemia in 1218 women with polycystic ovary syndrome. *Endocrine.* 2014;**47**(2):631-638.

15. Abbott DH, Dumesic DA, Levine JE. Hyperandrogenic origins of polycystic ovary syndrome - implications for pathophysiology and therapy. *Expert Rev Endocrinol Metab.* 2019;**14**(2):131-143.

16. Walters KA, Rodriguez Paris V, Aflatounian A, Handelsman DJ. Androgens and ovarian function: translation from basic discovery research to clinical impact. *J Endocrinol.* 2019;**242**(2):R23-R50.

17. Kataoka J, Tassone EC, Misso M, et al. Weight management interventions in women with and without PCOS: a systematic review. *Nutrients.* 2017;**9**(9):996.

18. Escobar-Morreale HF, San Millán JL. Abdominal adiposity and the polycystic ovary syndrome. *Trends Endocrinol Metab.* 2007;**18**(7):266-272.

19. Gambineri A, Pelusi C, Vicennati V, Pagotto U, Pasquali R. Obesity and the polycystic ovary syndrome. *Int J Obes Relat Metab Disord.* 2002;**26**(7):883-896.

20. Moran LJ, Ko H, Misso M, et al. Dietary composition in the treatment of polycystic ovary syndrome: a systematic review to inform evidence-based guidelines. *J Acad Nutr Diet.* 2013;**113**(4):520-545.

21. Lim SS, Norman RJ, Davies MJ, Moran LJ. The effect of obesity on polycystic ovary syndrome: a systematic review and meta-analysis. *Obes Rev.* 2013;**14**(2):95-109.

22. Elbers JMH, Asscheman H, Seidell JC, Megens JAJ, Gooren LJG. Long-term testosterone administration increases visceral fat in female to male transsexuals. *J Clin Endocrinol Metab.* 1997;**82**(7):2044-2047.

23. Koivuaho E, Laru J, Ojaniemi M, et al. Age at adiposity rebound in childhood is associated with PCOS diagnosis and obesity in adulthood—longitudinal analysis of BMI data from birth to age 46 in cases of PCOS. *Int J Obes.* 2019;**43**(7):1370-1379.

24. de Zegher F, López-Bermejo A, Ibáñez L. Central obesity, faster maturation, and 'PCOS' in girls. *Trends Endocrinol Metab.* 2018;**29**(12):815-818.

25. Ibáñez L, de Zegher F. Polycystic ovary syndrome in adolescent girls. *Pediatr Obes.* 2020;**15**(2):e12586.

26. Malpique R, Sánchez-Infantes D, Garcia-Beltran C, et al. Towards a circulating marker of hepato-visceral fat excess: S100A4 in adolescent girls with polycystic ovary syndrome—evidence from randomized clinical trials. *Pediatr Obes.* 2019;**14**(5):e12500.

27. Walters KA, Bertoldo MJ, Handelsman DJ. Evidence from animal models on the pathogenesis of PCOS. *Best Pract Res Clin Endocrinol Metab.* 2018;**32**(3):271-281.

28. Stener-Victorin E, Padmanabhan V, Walters KA, et al. Animal models to understand the etiology and pathophysiology of polycystic ovary syndrome. *Endocr Rev.* 2020;**41**(4):538-576.

29. Mannerås L, Cajander S, Holmäng A, et al. A new rat model exhibiting both ovarian and metabolic characteristics of polycystic ovary syndrome. *Endocrinology.* 2007;**148**(8):3781-3791.

30. Caldwell ASL, Edwards MC, Desai R, et al. Neuroendocrine androgen action is a key extraovarian mediator in the development of polycystic ovary syndrome. *Proc Natl Acad Sci.* 2017;**114**(16):E3334-E3343.

31. Leonie E, van Houten AF, Kramer P, et al. Reproductive and metabolic phenotype of a mouse model of PCOS. *Endocrinology.* 2012;**153**(6):2861-2869.

32. Caldwell AS, Middleton LJ, Jimenez M, et al. Characterization of reproductive, metabolic, and endocrine features of polycystic ovary syndrome in female hyperandrogenic mouse models. *Endocrinology.* 2014;**155**(8):3146-3159.

33. Bertoldo MJ, Caldwell ASL, Riepsamen AH, et al. A hyperandrogenic environment causes intrinsic defects that are detrimental to follicular dynamics in a PCOS mouse model. *Endocrinology.* 2019;**160**(3):699-715.

34. Cox MJ, Edwards MC, Rodriguez Paris V, et al. Androgen action in adipose tissue and the brain are key mediators in the development of PCOS traits in a mouse model. *Endocrinology.* 2020;**161**(7):bqaa061.

35. Singh J, O'Neill C, Handelsman DJ. Induction of spermatogenesis by androgens in gonadotropin-deficient (hpg) mice. *Endocrinology.* 1995;**136**(12):5311-5321.

36. Aflatounian A, Edwards MC, Rodriguez Paris V, et al. Androgen signaling pathways driving reproductive and metabolic phenotypes in a PCOS mouse model. *J Endocrinol.* 2020;**245**(3):381-395.

37. Rodriguez Paris V, Solon-Biet SM, Senior AM, et al. Defining the impact of dietary macronutrient balance on PCOS traits. *Nat Commun.* 2020;**11**(1):5262.

38. Walters KA, Middleton LJ, Joseph SR, et al. Targeted loss of androgen receptor signaling in murine granulosa cells of preantral and antral follicles causes female subfertility. *Biol Reprod.* 2012;**87**(6):151.

39. Walters KA, Allan CM, Jimenez M, et al. Female mice haploinsufficient for an inactivated androgen receptor (AR) exhibit age-dependent defects that resemble the AR null phenotype of dysfunctional late follicle development, ovulation, and fertility. *Endocrinology.* 2007;**148**(8):3674-3684.

40. Myers M, Britt KL, Wreford NG, Ebling FJ, Kerr JB. Methods for quantifying follicular numbers within the mouse ovary. *Reproduction.* 2004;**127**(5):569-580.

41. Kleiner DE, Brunt EM, Van Natta M, et al.; Nonalcoholic Steatohepatitis Clinical Research Network. Design and validation of a histological scoring system for nonalcoholic fatty liver disease. *Hepatology.* 2005;**41**(6):1313-1321.

42. Dumesic DA, Akopians AL, Madrigal VK, et al. Hyperandrogenism accompanies increased intra-abdominal fat storage in normal weight polycystic ovary syndrome women. *J Clin Endocrinol Metab.* 2016;**101**(11):4178-4188.

43. Legro RS, Kunselman AR, Dunaif A. Prevalence and predictors of dyslipidemia in women with polycystic ovary syndrome. *Am J Med.* 2001;**111**(8):607-613.

44. Hall P, Cash J. What is the real function of the liver 'function' tests? *Ulster Med J.* 2012;**81**(1):30-36.

45. Azziz R, Sanchez LA, Knochenhauer ES, et al. Androgen excess in women: experience with over 1000 consecutive patients. *J Clin Endocrinol Metab.* 2004;**89**(2):453-462.

46. Ankarberg C, Norjavaara E. Diurnal rhythm of testosterone secretion before and throughout puberty in healthy girls: correlation with 17β-estradiol and dehydroepiandrosterone sulfate. *J Clin Endocrinol Metab.* 1999;**84**(3):975-984.

47. Risal S, Pei Y, Lu H, et al. Prenatal androgen exposure and transgenerational susceptibility to polycystic ovary syndrome. *Nat Med.* 2019;**25**(12):1894-1904.

48. Dumesic DA, Akopians AL, Madrigal VK, et al. Hyperandrogenism accompanies increased intra-abdominal fat storage in normal weight polycystic ovary syndrome women. *J Clin Endocrinol Metab.* 2016;**101**(11):4178-4188.

49. Lord J, Thomas R, Fox B, Acharya U, Wilkin T. The central issue? visceral fat mass is a good marker of insulin resistance and metabolic disturbance in women with polycystic ovary syndrome. *Bjog.* 2006;**113**(10):1203-1209.

50. Christensen SB, Black MH, Smith N, et al. Prevalence of polycystic ovary syndrome in adolescents. *Fertil Steril.* 2013;**100**(2):470-477.

51. Laitinen J, Taponen S, Martikainen H, et al. Body size from birth to adulthood as a predictor of self-reported polycystic ovary syndrome symptoms. *Int J Obes Relat Metab Disord.* 2003;**27**(6):710-715.

52. Abarca-Gómez L, Abdeen ZA, Hamid ZA, et al. Worldwide trends in body-mass index, underweight, overweight, and obesity from 1975 to 2016: a pooled analysis of 2416 population-based measurement studies in 128·9 million children, adolescents, and adults. *Lancet.* 2017;**390**(10113):2627-2642.

53. Legro RS. Obesity and PCOS: implications for diagnosis and treatment. *Semin Reprod Med.* 2012;**30**(6):496-506.

54. Demirel F, Bideci A, Cinaz P, et al. Serum leptin, oxidized low density lipoprotein and plasma asymmetric dimethylarginine levels and their relationship with dyslipidaemia in adolescent girls with polycystic ovary syndrome. *Clin Endocrinol (Oxf).* 2007;**67**(1):129-134.

55. Diamanti-Kandarakis E, Papavassiliou AG, Kandarakis SA, Chrousos GP. Pathophysiology and types of dyslipidemia in PCOS. *Trends Endocrinol Metab.* 2007;**18**(7):280-285.

56. Rossi B, Sukalich S, Droz J, et al. Prevalence of metabolic syndrome and related characteristics in obese adolescents with and without polycystic ovary syndrome. *J Clin Endocrinol Metab.* 2008;**93**(12):4780-4786.

57. Patel SS, Truong U, King M, et al. Obese adolescents with polycystic ovarian syndrome have elevated cardiovascular disease risk markers. *Vasc Med.* 2017;**22**(2):85-95.

58. Dahan MH, Reaven G. Relationship among obesity, insulin resistance, and hyperinsulinemia in the polycystic ovary syndrome. *Endocrine.* 2019;**64**(3):685-689.

59. Garber AJ, Abrahamson MJ, Barzilay JI, et al. Consensus statement by the American Association of Clinical Endocrinologists and American College of Endocrinology on the comprehensive type 2 diabetes management algorithm—2019 executive summary. *Endocr Pract.* 2019;**25**(1):69-100.

60. Kumarendran B, O'Reilly MW, Manolopoulos KN, et al. Polycystic ovary syndrome, androgen excess, and the risk of nonalcoholic fatty liver disease in women: A longitudinal study based on a United Kingdom primary care database. *Plos Med.* 2018;**15**(3):e1002542.

61. Ayonrinde OT, Adams LA, Doherty DA, et al. Adverse metabolic phenotype of adolescent girls with non-alcoholic

fatty liver disease plus polycystic ovary syndrome compared with other girls and boys. *J Gastroenterol Hepatol.* 2016;**31**(5):980-987.

62. Goessling W, Massaro JM, Vasan RS, D'Agostino RB Sr, Ellison RC, Fox CS. Aminotransferase levels and 20-year risk of metabolic syndrome, diabetes, and cardiovascular disease. *Gastroenterology.* 2008;**135**(6):1935-44, 1944.e1.

63. Petta S, Ciresi A, Bianco J, et al. Insulin resistance and hyperandrogenism drive steatosis and fibrosis risk in young females with PCOS. *Plos One.* 2017;**12**(11):e0186136.